processes

MDPI

Article

Solvent Extraction of Gold(III) by 2-Ethylhexanol and Modeling of Facilitated Transport across a Supported Liquid Membrane

Francisco Jose Alguacil * and Jose Ignacio Robla *

Centro Nacional de Investigaciones Metalurgicas (CSIC), Avda. Gregorio del Amo 8, 28040 Madrid, Spain
* Correspondence: fjalgua@cenim.csic.es (F.J.A.); jrobla@cenim.csic.es (J.I.R.)

Abstract: The solvent extraction of gold(III) by undiluted 2-ethylhexanol or dissolved in toluene from a HCl solution has been investigated in this paper. The numerical analysis of gold distribution data suggests the formation of $HAuCl_4 \cdot L$ and $HAuCl_4 \cdot 2L$ (L = 2-ethylhexanol) species in the organic phase, with formation constants K_{11} = 38 and K_{12} = 309, respectively. The results derived from gold(III) distribution have been implemented in a solid-supported liquid membrane system. The influence of several variables on gold transport has been considered: feed and receiving phases' stirring speeds, HCl and gold concentrations in the feed phase, and carrier concentration in the membrane phase as well as the presence of base metals (Fe, Cu, Ni) and platinum-group metals (PGMs) in the feed phase. Gold transport is influenced by the stirring speed of the feed phase and the variation in HCl and gold (feed phase) and carrier (membrane phase) concentrations. Also, diffusional resistances to mass transfer are estimated, and the contribution of each resistance to gold transport is estimated. Gold is recovered as zero-valent nanoparticles.

Keywords: gold(III); 2-ethylhexanol; extraction; membrane transport; gold nanoparticles

Citation: Alguacil, F.J.; Robla, J.I. Solvent Extraction of Gold(III) by 2-Ethylhexanol and Modeling of Facilitated Transport across a Supported Liquid Membrane. *Processes* **2024**, *12*, 771. https://doi.org/10.3390/pr12040771

Academic Editors: Yanlin Zhang and Prashant K. Sarswat

Received: 29 February 2024
Revised: 9 April 2024
Accepted: 9 April 2024
Published: 11 April 2024

1. Introduction

Over the last few years, there has been an increasing interest in the recovery and utilization of so-called strategic metals (rare earth elements, lithium, neodymium, tantalum, etc.); less mentioned was the recovery, from secondary materials or waste, of gold and platinum-group metals, which have always been of interest.

The recovery of gold has two main tendencies: (i) recovery from raw materials, which is dominated by cyanidation and gold adsorption, and (ii) recovery from secondary materials or waste (printed circuit boards, jewelry scraps, e-waste, etc.), in which the precious metal is usually dissolved in a non-cyanide medium, i.e., aqua regia, thiourea, thiosulphate, etc. From the leachates, gold is purified and recovered via different options.

Though yet with no apparent or definitive practical applications, the scientific community has considered the recovery of gold from these various non-cyanide media important, an importance which is reflected by the series of publications which, every year, appear in journals. With respect to gold adsorption onto different materials, several recent approaches have been considered, including the use of metal organic frameworks [1], metal sulfide microspheres [2], or Aliquat 336 (quaternary ammonium salt) impregnating a Nitrolite adsorbent [3].

The recovery of metals by solvent extraction processing is well known; this is also demonstrated by the number of publications on the subject over the years. Gold(III) solvent extraction has attracted interest, with recent publications discussing the use of ionic liquids [4] or pseudo-protic ionic liquids [5] as extractants for this precious metal.

Due to some environmental and operational concerns (i.e., solvent extraction is not adequate in the treatment of dilute solutions), liquid membranes have emerged as an alternative to solvent extraction; however, it must be said that, at the present time, there is still no plant using any of the different liquid membrane operational variations. Indeed, the interest of scientists in the utilization of these membranes technologies on the recovery of

metals or other pollutants is still alive, as some recent publications have also demonstrated. Several reviews about the general use of liquid membranes included the transport of actinide elements using diglycolamides as carriers [6] and the application of membranes in the recovery of various elements [7–10], with a mention of the use of polymer inclusion membranes (PIMs) [11]. Experimental papers have been devoted to investigating the transport of both inorganic and organic solutes or harmful species potentially appearing in liquid waste. As organic compounds, the transport of diclofenac and ibuprofen by supported liquid membrane technology and Cyanex 923 (mixture of tri-alkylphosphine oxides) dissolved in kerosene as the carrier phase has been investigated [12,13]. Using a flat-sheet, supported liquid membrane operational mode, the transport of chromium(VI), indium(III), and the separation of Nd(III) and Er(III) have been investigated [14–16]; a variation of the above operation has been found in the investigation of the transport process (copper, zinc, or cobalt) using electromembranes [17–19].

The utilization of a more dynamic, supported liquid membrane procedure, such as the use of hollow fiber modules, has found applications in the simultaneous removal of arsenic and mercury [20] or only mercury [21]. A yet-more-advanced hollow fiber application is the so-called (though other names have been used) pseudo-emulsion-based hollow fiber membrane with strip-dispersion technology (PEHFMSD), in which, differently to conventional hollow fiber use, employing two modules (one for extraction and another for stripping), just one module is used for extraction and stripping. Moreover, in this PEHFMSD process, the organic and the receiving or stripping phase are mixed in one tank and continuously pumped into the module to improve the transport and removal of the solute from the feed to the organic and from the organic to the receiving phases. This PEHFMSD process was recently used in the removal of iron(III) [22] and in the treatment of stainless steel rinse waters [23]. It is worth noting that, against all the literature favoring the use of liquid membranes in the treatment of wastewaters, these technologies seem unpopular in the case of acid mine wastewater treatment [24].

In the application of these membranes, it is of the utmost importance to gain knowledge on the interfacial phenomena associated with metal carrier's (extractant) chemical reactions occurring in the feed phase and the membrane interfaces when the metal (solute) is transported against its concentration gradient. Before scaling up the use of flat-sheet, supported liquid membranes (the simplest form of supported liquid membranes) to spiral wound or hollow fiber module operational modes, a theoretical model of the membrane system is welcomed to design an efficient and stable process.

The present work implemented solvent extraction investigations in a solid, supported liquid membrane configuration. Firstly, a quantitative characterization of the solvent extraction of gold(III) by 2-ethylhexanol was undertaken. Further, a liquid membrane system was designed using the extraction process mentioned above, and the parameters affecting the liquid membrane—stirring speeds applied in both feed and receiving phases, composition of the feed and organic phases, etc.—were investigated. A model was developed to estimate the mass transfer coefficients relative to the transport of gold across the 2-ethylhexanol-immobilized supported liquid membrane.

2. Materials and Methods

2.1. Materials

A stock solution (1 g/L) of gold(III) was prepared by dissolving $HAuCl_4$ (Fluka, Buchs, Switzerland) in HCl. The aqueous solutions for solvent extraction or the membrane transport experiments were prepared by the dilution of this stock solution. The extractant 2-ethylhexanol (Merck, Rahway, NJ, USA) was used without further purification. The PGM stock solution was a commercially available standard solution for ICP analysis. All the other reagents used in this investigation were of AR grade.

The support for the liquid membrane was a polydifluoroethylene film (Millipore GVHP4700, Darmstadt, Germany) with a thickness of 125×10^{-4} cm, a porosity of 75%, a tortuosity of 1.67, and a 0.22 μm average pore size.

2.2. Methods

2.2.1. Liquid–Liquid Extraction Experiments

Before experimentation, undiluted 2-ethylhexanol was pre-saturated with 6 M HCl in order to avoid a change in the organic and aqueous phases' volume after gold extraction, and, from this pre-saturated alcoholic solution, all the organic phases used in the investigation were prepared. Distribution ratio experiments were performed at 20 °C by shaking (800 min^{-1}) equal volumes (25 cm^3) of the aqueous and organic phases in glass separatory funnels for the required time. After phase separation, the metal remaining in the raffinate was analyzed by AAS (±2.5 reproducibility) using a Perkin Elmer 1100B (Waltham, MA, USA) spectrophotometer. The amount of metals extracted in the organic phase was calculated by the difference with the initial concentration in the aqueous phase. The percentage of extraction was calculated as follows:

$$\%E = \frac{[M]_{aq,0} - [M]_{aq,t}}{[M]_{aq,0}} \times 100 \quad (1)$$

where $[M]_{aq,0}$ and $[M]_{aq,t}$ are the metal concentrations in the initial aqueous phase and in the raffinate, respectively.

2.2.2. Liquid Membrane Experiments

The batch transport experiments were carried out in a methacrylate permeation cell having two (200 cm^3 each) compartments separated by a solid support (Figure 1). One compartment was for the feed phase and the other for the receiving or stripping phase. The liquid membrane was prepared by impregnation of the laminar microporous support by the carrier phase over 24 h and then by leaving it to drip for twenty seconds before placing it in the cell. The metal contents in the feed and receiving phases were periodically analyzed by AAS or ICP (platinum-group metals) (±1.5 reproducibility), whereas the overall mass transfer coefficient (K_0) was calculated as follows:

$$\ln\frac{[M]_{f,t}}{[M]_{f,0}} = -\frac{A}{V}K_0 t \quad (2)$$

where $[M]_{f,0}$ and $[M]_{f,t}$ are the metal concentrations in the feed at time zero and at an elapsed time, respectively; A is the effective membrane area 11.3 cm^2; V is the volume of the feed phase (200 cm^3); and t is the elapsed time.

Figure 1. Permeation cell. A: feed phase; B: membrane support; and C: stripping phase.

3. Results and Discussion

3.1. Solvent Extraction Experiments

Firstly, the influence of the equilibration time on the attachment gold(III) extraction equilibrium was studied. In these series of experiments, the aqueous phase contained 35 g/L Au(III) in 6 M HCl, whereas the organic phase was of 75% v/v 2-ethylhexanol in toluene. From the results shown in Table 1, it can be concluded that equilibrium was almost reached within 2 min of contact between both phases, and the same conclusion was reached when the aqueous phase contained other (15–100 g/L) gold concentrations.

Table 1. Influence of equilibration time on the fractional attachment to the equilibrium.

Time, min	F
1	0.71
2	0.98
5	1
10	1
15	1

Temperature: 20 °C. Org/Aq volume ratio: 1.

In Table 1, the fractional attachment to the equilibrium (F) was calculated as follows:

$$F = \frac{[Au]_{org,t}}{[Au]_{org,e}} \quad (3)$$

where $[Au]_{org,t}$ and $[Au]_{org,e}$ are the gold concentrations in the organic phase at an elapsed time and at the equilibrium, respectively. According to these experimental data, all the subsequent experiments were carried out over 5 min of contact between the respective organic and aqueous phases.

The variation in the initial gold concentration from the extraction of this precious metal from a 6 M HCl medium was also investigated. In these cases, the initial aqueous solutions contained varying gold concentrations in the 5–200 g/L range, and the organic phases were of undiluted 2-ethylhexanol. The results from this set of experiments are shown in Table 2.

Table 2. Percentage of gold extraction at various initial metal concentrations in the aqueous phase.

$[Au]_0$, g/L	% Extraction
5	98
15	98
25	98
35	98
50	98
75	97
100	96
150	93
200	87

Temperature: 20 °C. Org/Aq volume ratio: 1.

These results concluded that, in the 5–100 g/L gold concentration range, the variation in the percentage of gold extraction during the organic phase was almost negligible (96–98%), whereas, at higher initial gold concentrations, in the aqueous solutions, these percentages decreased from 93% at a 100 g/L gold concentration to 87% at a 200 g/L gold concentration. This decrease in the percentage of gold extraction with the increase in the initial metal concentration is not rare [25–28] and can be due to the polymerization of the metal in the aqueous phase and also to the common ion effect, according to which the organic phase is dominated by the metal anion ($AuCl_4^-$ in this work) and the aqueous phase by the halide ions (Cl^- in this case) [29].

The influence of the variation in the initial extractant concentration on gold extraction was also investigated using organic phases containing 25–90% *v*/*v* 2-ethylhexanol in toluene or an undiluted extractant. The aqueous phase was 35 g/L Au(III) in a 6 M HCl medium; the results from these experiments are shown in Table 3.

Table 3. Percentage of gold extraction at various extractant concentrations in the organic phase.

[2-Ethylhexanol], % *v*/*v*	% Extraction
25	57
35	75
50	88
60	92
70	94
75	95
80	96
90	98
undiluted	98

Temperature: 20 °C. Org/Aq volume ratio: 1.

These results indicated that there was an increase in the percentage of gold extraction with the increase in the extractant concentration in the organic phase from 25 to 60% *v*/*v*, though, for extractant concentrations higher than 70% *v*/*v*, the variation in gold extraction did not exceed 5%.

The stoichiometry of the extracted species and their equilibrium constants were determined through the treatment of the experimental data using a numerical program, which minimized the U function, defined as follows:

$$U = \sum \log(D_{cal} - D_{exp})^2 \quad (4)$$

where D_{cal} and D_{exp} are the respective distribution ratios calculated from the mass balance equations for the various models, experimentally calculated as

$$D_{exp} = \frac{[Au]_{org}}{[Au]_{aq}}. \quad (5)$$

The results of the numerical treatment indicated that the extraction of gold(III) can be explained (U = 0.009) by the formation of $HAuCl_4 \cdot L$ ($\log K_{ext} = 1.58 \pm 0.09$) and $HAuCl_4 \cdot 2L$ ($\log K_{ext} = 2.49 \pm 0.26$) species in the gold-loaded organic phases. In the above formulations, L represents 2-ethylhexanol molecules.

Once gold had been extracted in the organic phase, a stripping operation was performed using water as the stripping agent. In this case, from an organic phase of undiluted 2-ethylhexanol containing 34 g/L gold, using the same volume of water (Org/Aq = 1), near 89% of gold was recovered at 20 °C in one step. From these solutions, gold can be recovered by precipitation with sodium borohydride, oxalic acid, etc.; however, this last step was not investigated in our study, unlike in the case of solutions derived from supported liquid membrane experimentation (see further).

The selectivity of the present system against the presence of Cu(II), Zn(II), and Ni(II) in the aqueous phase was also investigated. These experiments used organic phases of undiluted 2-ethylhexanol and aqueous phases containing, separately, 0.18 M of the element in 6 M HCl. The results from this set of experiments are summarized in Table 4.

The separation factor (SF) values showed the extreme selectivity of the system; these separation factors were calculated using the following equation:

$$SF = \frac{D_{Au}}{D_M}. \quad (6)$$

Table 4. Extraction of Au(III), Cu(II), Fe(III), and Ni(II).

Element	% Extraction	D	SF
Au(III)	98	69	
Cu(II)	21	0.25	276
Zn(II)	11	0.12	575
Ni(II)	12	0.13	530

Temperature: 20 °C. Org/Aq volume ratio: 1.

Further experiments were performed to explain the separation of Au(III)/Cu(II) using this same organic phase, an aqueous phase containing both elements in 6 M HCl, and various Au(III):Cu(II) molar concentration ratios. Table 5 summarizes these results.

Table 5. Extraction and separation of Au(III) and Cu(II) at various molar concentration ratios.

$[Au]_0$:$[Cu]_0$	D_{Au}	D_{Cu}	SF
2:1	69	0.045	1533
3:1	69	0.047	1468
6:1	69	0.044	1568
18:1	69	0.049	1408

$[Au]_0$: 0.18 M; temperature: 20 °C; and Org/Aq volume ratio: 1.

These results show that, in mixed Au(III)-Cu(II) solutions, the extraction of this last element decreased with respect to the results obtained from the use of single-metal-bearing solutions. This is why the SF values resulted to be in the 1400–1500 order, though the variation in the $[Au(III)]_0$:$[Cu(II)]_0$ ratio did not seem to greatly influence this separation.

3.2. Supported Liquid Membrane Experiments

In these membrane systems, the extraction (transport) of a given metal species depends not only on the equilibrium parameters but also on the kinetics parameters.

The influence of the variation (600–1600 rpm) in the stirring speed of the feed phase on gold transport was investigated. The results from these experiments are shown in Table 6, and it can be observed that the overall mass transfer coefficient value (K_O) increased with the increase in the stirring speed from 600 to 1000 rpm, and, beyond that, no increase in gold transport was observed. In fact, there was a decrease in transport from 1400 rpm due to membrane instability, probably attributable to the displacement of the organic phase from the membrane pores caused by the turbulence from these higher stirring speeds.

Table 6. Influence of the feed-phase stirring speed on gold transport.

Stirring Speed, rpm	$K_O \times 10^3$, cm/s
600	0.95
800	2.6
1000	5.7
1200	5.7
1400	5.5
1600	4.9

Feed phase: 0.01 g/L Au(III) in 6 M HCl. Membrane phase: 50% *v*/*v* 2-ethylhexanol in toluene immobilized on GVHP4700 support. Receiving phase: water. Receiving-phase stirring speed: 1200 rpm. Temperature: 20 °C.

In supported liquid membrane experimentation, two types of diffusional resistance are usually found: (i) one due to the feed-phase boundary layer, and (ii) another in relation to the membrane support. Often, the magnitudes of the values of both resistances compete between them [30]. These experimental results show that, in the 1000–1200 rpm range, the feed-phase boundary layer reaches a minimum, the aqueous resistance to mass transfer should be minimized, and, thus, the diffusion contribution of the aqueous species to mass transfer phenomena is constant [31].

The influence of the variation (800–1200 rpm) in the stirring speed of the receiving phase on gold transport was also investigated using the same experimental conditions as in Table 6 but with a stirring speed of 1000 rpm in the feed phase. The results from these experiments showed that the variation in the stirring speed applied to the receiving phase had a negligible influence on gold transport. In the case of the receiving phase and if the stirrer in the receiving compartment was close to the support, the thickness of the boundary layer was minimized, and the resistance in the receiving side was neglected [32]. Thus, subsequent experiments were performed using stirring speeds of 1000 rpm for both feed and receiving phases.

Another variable investigated was the variation (0.5–6 M) in the HCl concentration in the feed phase on gold transport, keeping the carrier concentration in the membrane support constant. The results are shown in Table 7. It can be seen that gold permeation increased when the acid concentration in the feed solution was increased up to 1 M, with metal permeation being independent of the HCl concentration in the 3–6 M range due to the following equilibrium:

$$HAuCl_4 \leftrightarrow AuCl_4^- + H^+ \quad (7)$$

where the equilibrium is shifted completely to the left, and $HAuCl_4$ is the predominant species in the feed solution.

Table 7. Gold(III) permeation at various HCl concentrations in the feed phase.

[HCl], M	$K_O \times 10^3$, cm/s
0.5	3.8
1	4.7
3	5.7
6	5.7

Feed phase: 0.01 g/L Au(III) and HCl. Membrane phase: 50% *v*/*v* 2-ethylhexanol in toluene immobilized on GVHP4700 support. Receiving phase: water. Temperature: 20 °C.

The influence of the variation in the carrier concentration on gold transport was investigated next. In these experiments, the feed phase was 0.01 g/l Au(III) in 6 M HCl, whereas the organic phase contained 10–75% *v*/*v* 2-ethylhexanol in toluene or undiluted extractant. Table 8 shows the variation in the overall mass transfer coefficient with the variation in the carrier concentration in the membrane phase.

Table 8. Gold transport at various carrier concentrations.

[Carrier], % *v*/*v*	$K_O \times 10^3$, cm/s	[a] % Gold Recovery
10	1.2	95
25	2.7	95
35	4.0	94
45	5.6	93
50	5.7	92
65	5.5	93
75	3.0	90
undiluted	1.2	89

Membrane support: GVHP4700. Receiving phase: water. [a] In the receiving phase, after 3 h.

These results demonstrated that gold transport increased from 10 to 50% *v*/*v* carrier concentration in the membrane phase, then leveled off, and, after, decreased at the highest carrier concentrations. These phenomena could be attributed to the fact that, at low carrier concentrations, metal transport was dominated by membrane diffusion, whereas, in the 50% *v*/*v* range, the contribution of membrane diffusion was negligible and gold transport was controlled by the diffusion in the stagnant film of the feed phase. At this maximum K_O value [33],

$$K_O = \frac{D_{aq}}{d_{aq}} \quad (8)$$

where D_{aq} represents the average aqueous diffusion coefficient (10^{-5} cm^2/s) of the metal species in the feed phase [34], and d_{aq} is the minimum thickness of the feed phase boundary layer. Thus, d_{aq}, for the present system, was estimated at 1.8×10^{-3} cm. The decrease in gold transport at the highest carrier concentration was due to the increase in the organic-phase viscosity, which decreased the Au(III)-2-ethylhexanol complexes' diffusion coefficients values [35]. Moreover, the diffusion coefficients of the gold carrier species in the membrane phase were calculated as follows [36]:

$$D_{org,Au} = \frac{J \cdot d_{org}}{[carrier]} \quad (9)$$

The results are summarized in Table 9. In this equation, J is the metal flux (Equation (10)), and d_{org} is the thickness of the membrane support (125×10^{-4} cm). It can be seen that the increase in the carrier concentration was accompanied by a decrease in the diffusion coefficient and, thus, a decrease in the corresponding value of the overall permeation coefficient (Table 8).

Table 9. Variation in the diffusion coefficient in the membrane phase with the carrier concentration.

Carrier Concentration, %*v*/*v* (M)	$D_{org,Au} \times 10^9$, cm^2/s
50 (3.2)	1.1
65 (4.2)	0.83
75 (4.8)	0.39
Undiluted (6.4)	0.12

During our investigation on the effect of the initial concentration (0.01–0.1 g/L) of gold, in the feed phase, on metal transport (Table 10), it was observed that the increase in the initial gold concentration was accompanied by a continuous decrease in metal transport, whereas the initial metal flux (J) was defined as follows:

$$J = K_O[Au]_0 \quad (10)$$

It initially increased from 0.005 to 0.04 g/L in the initial gold concentrations, and, beyond this concentrations range, J became almost independent of the initial gold concentration in the feed phase.

Table 10. Variation in gold transport and initial flux at various metal concentrations.

$[Au]_0$, g/L	$K_O \times 10^3$, cm/s	J, mol/cm^2s	[a] % Gold Recovery
0.01	5.7	2.9	95
0.02	4.5	4.6	93
0.04	3.0	6.0	94
0.06	2.2	6.6	93
0.08	1.7	6.8	94
0.1	1.4	7.0	95

Feed phase: gold(III) in 6 M HCl. Membrane phase: 50% *v*/*v* 2-ethylhexanol in toluene immobilized on GVHP4700 support. Receiving phase: water. [a] In the receiving phase, after 3 h.

According to these results, at low metal concentrations (0.01–0.04 g/L), the transport process was controlled by the diffusion of gold species, whereas, in the highest metal concentrations range, the near-constant metal flux values were due to a change in the rate-determining step for the transport process. At these higher gold concentrations, the

membrane became saturated by metal carrier species on the feed membrane interface, resulting in a lower effective membrane area, which led to a near-constant initial flux value.

Following the same considerations described in the literature [37], it can be concluded that the gold transport rate was determined by the rate of diffusion of the $HAuCl_4$ species across the feed-phase diffusion layer and the rate of diffusion of the gold carrier species through the liquid membrane. Thus, making the same assumptions as [38,39], a final expression for the overall mass transfer coefficient can be derived as follows:

$$K_O = \frac{K_{11}\left[ROH\right]_{org} + K_{12}\left[ROH\right]^2_{org}}{\Delta_{org} + \Delta_f\left(K_{11}\left[ROH\right]_{org} + K_{12}\left[ROH\right]^2_{org}\right)} \quad (11)$$

where Δ_{org} and Δ_f are the transport resistances due to diffusion across the membrane and the aqueous feed boundary layer, respectively. The above equation combined, in one expression, both the equilibrium and diffusional parameters involved in the gold(III) transport process from the feed phase, across supported liquid membranes, using 2-ethylhexanol as the carrier.

To estimate the values of the resistance to the mass transfer, the above equation was linearized, resulting in the following:

$$\frac{1}{K_O} = \Delta_f + \Delta_{org}\frac{1}{K_{11}\left[ROH\right]_{org} + K_{12}\left[ROH\right]^2_{org}} \quad (12)$$

A plot of $1/K_O$ versus $1/(K_{11}\left[ROH\right]_{org} + K_{12}\left[ROH\right]^2_{org})$ might result in a straight line, with slope Δ_{org} and intercept Δ_f. From the plot, it resulted that Δ_{org} and Δ_f were 2580 s/cm and 147 s/cm, respectively, with r^2 = 0.9895. The utility of Equation (12) in describing gold transport across the supported liquid membrane by 2-ethylhexanol is shown in Figure 2, where the experimental values and those calculated using this equation have been represented against the initial carrier concentration.

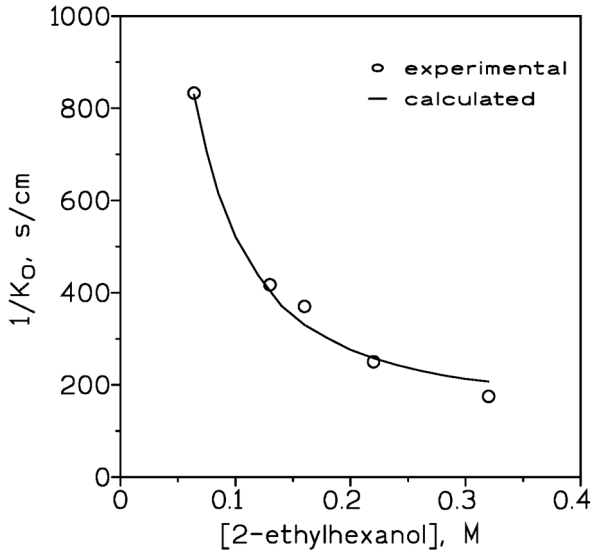

Figure 2. Plot of $1/K_O$ versus [2-ethylexanol]. Feed phase: 0.01 g/L Au(III) in 6 M HCl. Membrane phase: 10–50% *v*/*v* 2-ethylhexanol in toluene immobilized on GVHP4700. Receiving phase: water.

As the first term ($1/K_O$) of Equation (12) represents the value of the total resistance (R_T) and this resistance is the sum of the mass transfer resistances due to the feed and membrane phases, Equation (12) can be expressed as follows:

$$R_T = R_f + R_m. \quad (13)$$

The total resistance calculated from the experiments in Table 6 presented values in the 175–1052 s/cm range. In comparison, the total resistance calculated by the model is 206 s/cm, which indicates that the resistance due to the membrane is dominant at low stirring speeds.

The contribution of the fractional resistances due to each step of the total transport process, $R_f{}^o$ and $R_m{}^o$, can be expressed using the following equations:

$$\%R_f^o = \frac{R_f}{R_T} \times 100 \quad (14)$$

$$\%R_m^o = \frac{R_T - R_f}{R_T} \times 100. \quad (15)$$

The values of $\%R_f{}^o$ and $\%R_m{}^o$ under various experimental conditions are summarized in Table 11.

Table 11. Contribution of the mass transfer resistances to the gold(III) transport process.

Experimental Condition	R_T, s/cm	[a] R_T, s/cm	$\%R_f{}^o$	$\%R_m{}^o$
Carrier 10–50% *v*/*v*	370–175	147	40–84	60–16
Gold 0.01–0.1 g/L	175–714	147	84–21	16–79
HCl 6 M	175	147	84	16

[a] Value from the theoretical model (Equation (12)).

Taking into account that

$$D_{org} = \frac{d_m}{\Delta_{org}}, \quad (16)$$

where D_{org} represents the diffusion coefficient of the gold-containing species in the organic phase immobilized on the solid support and d_m is the membrane thickness, then, D_{org} is found to be 4.8×10^{-6} cm^2/s. The diffusion coefficient of the gold transported species in the bulk organic phase can be estimated using the following equation [40]:

$$D_{org,b} = \frac{D_{org}\tau^2}{\epsilon} \quad (17)$$

where τ and ε are the membrane tortuosity and porosity values, respectively. The above resulted in $D_{org,b}$ being calculated as 1.8×10^{-5} cm^2/s. A comparison of the D_{org} and $D_{org,b}$ values showed that D_{org} was lower than $D_{org,b}$, which can be attributed to the diffusional resistance caused by the solid support separating the feed and receiving phases.

The selectivity of the present system against the presence of other metals in the feed phase was investigated. In this case, the feed phase contained 0.01 g/L each of Au(III), Ni(II), Cu(II), Fe(III), and PGMs (Ir, Os, Pd, Pt, Re, Rh, and Ru) in a 6 M HCl medium, with the organic phase being 50% *v*/*v* 2-ethylhexanol in toluene immobilized on a Durapore GVHP4700 support. Like in all the previous experimentations, water was used as the receiving phase. The results indicated that PGMs were not transported under the present experimental conditions, whereas the transport of gold and base metals followed the Au(III) > Fe(III) > Cu(II) = Ni(III) order, with separation factors Au/Fe, Au/Ni, and Au/Cu of 1.3, 45, and 47, respectively. In these transport experiments, the separation factors were calculated as follows:

$$SF = \frac{K_{O,Au}}{K_{O,M}} \quad (18)$$

However, the presence of all these elements in the feed phase produced a decrease in the overall gold mass transfer coefficient, from 5.7×10^{-3} cm/s to 2.3×10^{-3} cm/s. This behavior is not rare in supported liquid membrane processes and is attributable to multi-ion competition or the crowding effect [41].

Once gold is transported from the feed solution to the membrane phase and, finally, to the receiving phase, it can be recovered from this last solution by precipitation as zero-

valent gold nanoparticles through the use of sodium borohydride. This procedure was used by one of the authors years ago [42]. The importance of the recovery of this precious metal in the form of nanoparticles has also been demonstrated [43], and the use of these nanoparticles in different fields (catalysis, medicine, sensors, etc.) has regularly appeared in the literature [44–47]. In the present work, the receiving solution containing 0.009 g/L gold was precipitated by the direct action of solid sodium borohydride, and, after the reaction had stopped, the dark solid was filtered. From this dry solid, the following images (Figures 3 and 4) were obtained.

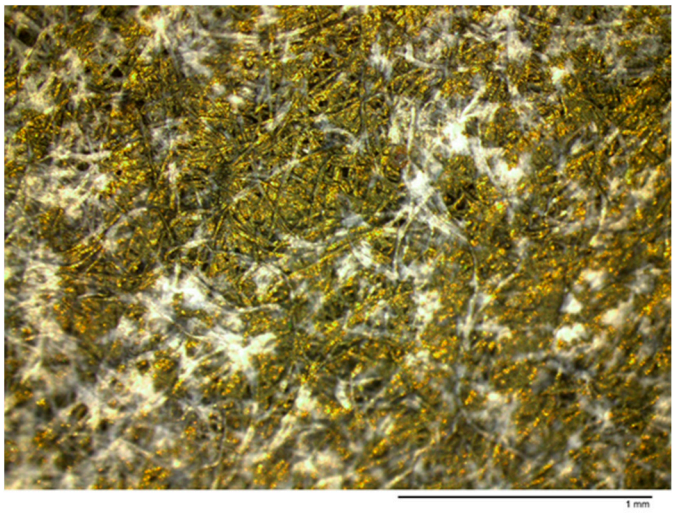

Figure 3. Gold nanoparticles under a magnifier.

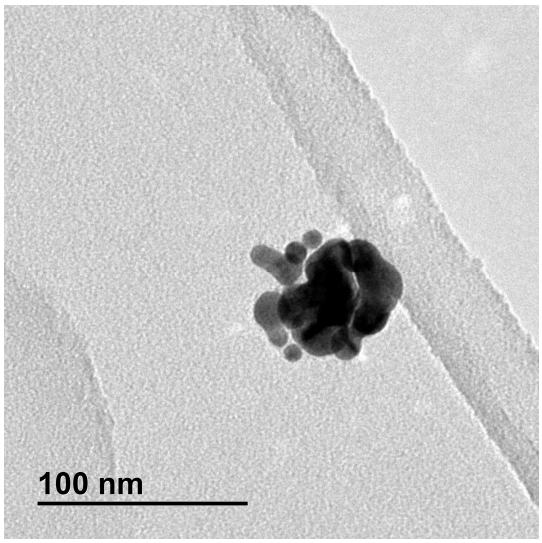

Figure 4. TEM image of gold nanoparticles. Some degree of agglomeration can be observed.

4. Conclusions

2-ethylhexanol was used to extract gold(III) from a 6 M HCl medium. The extraction process reached equilibrium within a few minutes, with metal extraction being dependent on gold and extractant concentrations. On the basis of numerical simulation, gold(III) extraction by 2-ethylhexanol can be explained by the formation of $HAuCl_4 \cdot L$ and $HAuCl_4 \cdot 2L$, with extraction constants of 38 and 309, respectively, and L being represented as the extractant molecule. The extraction process is highly selective with respect to gold(III) in the presence of copper(II), nickel(II), and zinc(II). Gold can be stripped from the metal-loaded organic phase with water.

The extraction system was implemented in a solid, supported liquid membrane system in which the metal flux was dependent on the initial gold concentration (up to 0.04 g/L) but almost independent from this variable above this concentration. The metal's transport was also dependent on the extractant's concentration, but, for 2-ethylhexanol concentrations in the 50% v/v range in toluene, a limiting value for the overall mass transfer coefficient was obtained. The mass transfer coefficients in the feed and membrane phases were calculated as 6.8×10^{-3} cm/s and 3.9×10^{-4} cm/s, respectively. The minimum thickness of the feed boundary layer was calculated to be 1.8×10^{-3} cm. The transport process was controlled by the mixed diffusion of gold across the feed phase and the diffusion of gold–2-ethylhexanol complexes in the liquid membrane phase. The system was selective with respect to Au(III) in the presence of platinum-group metals Cu(II) and Ni(II) in the aqueous feed phase and, to a lesser extent, with respect to the presence of Fe(III) in this phase as well (Au-Fe separation factor of 1.3). From the water-receiving phase, gold was recovered as zero-valent gold nanoparticles using sodium borohydride.

Author Contributions: Conceptualization, F.J.A.; methodology, F.J.A.; formal analysis, F.J.A.; investigation, F.J.A. and J.I.R.; writing—original draft preparation, F.J.A.; writing—review and editing, F.J.A. and J.I.R.; funding acquisition, J.I.R. All authors have read and agreed to the published version of the manuscript.

Funding: This research was funded by the CSIC-Project 202250E019.

Data Availability Statement: Data are contained within the article.

Acknowledgments: We would like to thank the CSIC (Spain) for the support and M.I. Maher for checking the English of this paper.

Conflicts of Interest: The authors declare no conflicts of interest.

References

1. Hu, G.; Wang, Z.; Zhang, W.; He, H.; Zhang, Y.; Deng, X.; Li, W. MIL-161 metal–organic framework for efficient Au(III) recovery from secondary resources: Performance, mechanism, and DFT calculations. *Molecules* **2023**, *28*, 5459. [CrossRef] [PubMed]
2. Zhao, L.; Zhou, Q.; Yang, Y.; Zhang, Y.; Qiu, Y.; Chen, Y.; Jin, X.; Yang, X.; Wang, S. Ultra-high adsorption capacity and selectivity of photo-enhanced sulfur-rich M2S3 (M[dbnd]Bi and Sb) for gold recovery from electronic wastewater. *J. Water Proc. Eng.* **2024**, *57*, 104572. [CrossRef]
3. Hubicki, Z.; Zinkowska, K.; Wójcik, G. A new impregnated adsorbent for noble metal ion sorption. *Molecules* **2023**, *28*, 6040. [CrossRef]
4. Thombre, A.V.; Kundu, D. Ionic liquid promoted extraction of gold(III) from electronic waste: A modeling study. *Sep. Sci. Technol.* **2023**, *58*, 2641–2654. [CrossRef]
5. Alguacil, F.J.; Robla, J.I. On the use of pseudo-protic ionic liquids to extract gold(III) from HCl solutions. *Int. J. Mol. Sci.* **2023**, *24*, 6305. [CrossRef] [PubMed]
6. Ansari, S.A.; Mohapatra, P.K. Diglycolamides as highly efficient carrier ligands for actinide transport in supported liquid membranes. *Desalin. Water Treat.* **2023**, *285*, 47–66. [CrossRef]
7. Botelho Junior, A.B.; Tenório, J.A.S.; Espinosa, D.C.R. Separation of critical metals by membrane technology under a circular economy framework: A review of the state-of-the-art. *Processes* **2023**, *11*, 1256. [CrossRef]
8. Kaczorowska, M.A. The latest achievements of liquid membranes for rare earth elements recovery from aqueous solutions—A mini review. *Membranes* **2023**, *13*, 839. [CrossRef]
9. Kostanyan, A.E.; Voshkin, A.A.; Belova, V.V.; Zakhodyaeva, Y.A. Modelling and comparative analysis of different methods of liquid membrane separations. *Membranes* **2023**, *13*, 554. [CrossRef]
10. Rzelewska-Piekut, M.; Regel-Rosocka, M. Liquid membranes for separation of metal ions from wastewaters. *Phys. Sci. Rev.* **2023**, *8*, 937–982. [CrossRef]
11. Wang, B.; Wang, H.; Yan, J.; Wang, Y.; Xu, T. Research progress of polymer inclusion membrane in metal separation and recovery. *Huagong Jinzhan Chem. Ind. Eng. Prog.* **2023**, *42*, 3990–4004. [CrossRef]
12. Farah, M.; Giralt, J.; Stüber, F.; Font, J.; Fabregat, A.; Fortuny, A. Hollow fiber liquid membrane: A promising approach for elimination of pharmaceutical compounds from wastewater. *J. Environ. Chem. Eng.* **2023**, *11*, 111544. [CrossRef]
13. Farah, M.; Giralt, J.; Stüber, F.; Font, J.; Fabregat, A.; Fortuny, A. Intensification of diclofenac removal through supported liquid membrane and ozonation. *Environ. Technol. Innov.* **2024**, *33*, 103469. [CrossRef]
14. Alguacil, F.J.; Robla, J.I. Transport of chromium(VI) across a aupported liquid membrane containing Cyanex 921 or Cyanex 923 dissolved in Solvesso 100 as carrier phase: Estimation of diffusional parameters. *Membranes* **2023**, *13*, 177. [CrossRef]

15. Kumar, R.; Dhiman, S.; Gupta, H. Indium extraction from nitrate medium using Cyphos ionic liquid 104 and its mathematical modeling. *Environ. Sci. Pollut. Res.* **2023**, *30*, 107341–107349. [CrossRef] [PubMed]
16. Middleton, A.; Hsu-Kim, H. Separation of rare-earth elements by supported liquid membranes: Impacts of soluble iron, aluminum, and pH in low-grade feedstocks. *ACS EST Eng.* **2023**, *3*, 1197–1204. [CrossRef]
17. Kadhim, N.R.; Abbar, A.H.; Flayeh, H.M. Removal of copper from a simulated wastewater by electromembrane extraction technique using a novel electrolytic cell provided with a flat polypropylene membrane infused with 1-octanol and DEHP as a carrier. *Case Stud. Chem. Environ. Eng.* **2023**, *8*, 100430. [CrossRef]
18. Kadhim, N.R.; Flayeh, H.M.; Abbar, A.H. Zinc (II) removal from simulated wastewater by electro-membrane extraction approach: Adopting an electrolysis cell with a flat sheet supported liquid membrane. *J. Electrochem. Sci. Eng.* **2023**, *13*, 1097–1112. [CrossRef]
19. Kadhim, N.R.; Flayeh, H.M.; Abbar, A.H. A new approach for cobalt (II) removal from simulated wastewater using electro membrane extraction with a flat sheet supported liquid membrane. *Heliyon* **2023**, *9*, e22343. [CrossRef] [PubMed]
20. Suren, S.; Punyain, W.; Maneeintr, K.; Nootong, K.; Pancharoen, U. The simultaneous elimination of arsenic and mercury ions via hollow fiber supported liquid membrane and their reaction mechanisms: Experimental and modeling based on DFT and generating function. *Arab. J. Chem.* **2023**, *16*, 104501. [CrossRef]
21. Traiwongsa, N.; Suren, S.; Pancharoen, U.; Nootong, K.; Maneeintr, K.; Punyain, W.; Lothongkum, A.W. Mechanisms of mercury ions separation by non-toxic organic liquid membrane via DFT, thermodynamics, kinetics and mass transfer model. *J. Ind. Eng. Chem.* **2023**, *117*, 522–537. [CrossRef]
22. Alguacil, F.J.; Robla, J.I. Iron control in liquid effluents: Pseudo-emulsion based hollow fiber membrane with strip dispersion technology with pseudo-protic ionic liquid ($RNH_3^+HSO_4^-$) as mobile carrier. *Membranes* **2023**, *13*, 723. [CrossRef] [PubMed]
23. Alguacil, F.J.; Robla, J.I. Treatment of stainless steel rinse waters using non-dispersive extraction and strip dispersion membrane technology. *Membranes* **2023**, *13*, 902. [CrossRef] [PubMed]
24. Wang, Y.; Cao, J.; Biswas, A.; Fang, W.; Chen, L. Acid mine wastewater treatment: A scientometrics review. *J. Water Proc. Eng.* **2024**, *57*, 104713. [CrossRef]
25. Pacary, V.; Burdet, F.; Duchesne, M.T. Experimental and modeling of extraction of lanthanides in system HNO_3-TEDGA-{DMDOHEMA-HDEHP}. *Proc. Chem.* **2012**, *7*, 328–333. [CrossRef]
26. Zhang, J.; Liu, R.; Liu, X.; Li, J.; Wu, R.; Yang, Y. Study on extraction of Rh(III) by DABCO-based ionic liquid from hydrochloric acid medium. *Sep. Purif. Technol.* **2023**, *324*, 124578. [CrossRef]
27. Li, H.; Mabhiza, T.; Ning, Y.; Yu, Z.; Lv, C.; Shen, X.; Wei, G.; Qu, J. Solvent extraction and recovery of beryllium from hydrochloric acid solution with naphthenic acid. *Sep. Purif. Technol.* **2024**, *331*, 125594. [CrossRef]
28. Dong, H.; Ci, E.; Zhao, T.; Chen, P.; Liu, F.; Hu, G.; Yang, L. Hydrophobic deep eutectic solvents as the green media for highly efficient extraction of Cr(VI) over a broad pH range and low oil-water ratio. *Sep. Purif. Technol.* **2024**, *334*, 126104. [CrossRef]
29. Diamond, R.M. The solvent extraction behavior of inorganic compounds. III. Variation of the distribution quotient with metal ion concentration. *J. Phys. Chem.* **1957**, *61*, 75–81. [CrossRef]
30. Bohrer, M.P. Diffusional boundary layer resistance for membrane transport. *Ind. Eng. Chem. Fundam.* **1983**, *22*, 72–78. [CrossRef]
31. Alguacil, F.J.; Martinez, S. Permeation of iron(III) by an immobilised liquid membrane using Cyanex 923 as mobile carrier. *J. Membr. Sci.* **2000**, *176*, 249–255. [CrossRef]
32. Pavón, S.; Fortuny, A.; Coll, M.T.; Bertau, M.; Sastre, A.M. Permeability dependencies on the carrier concentration and membrane viscosity for Y(III) and Eu(III) transport by using liquid membranes. *Sep. Purif. Technol.* **2020**, *239*, 116573. [CrossRef]
33. Alguacil, F.J.; Alonso, M.; Lopez, F.; Lopez-Delgado, A. Uphill permeation of Cr(VI) using Hostarex A327 as ionophore by membrane-solvent extraction processing. *Chemosphere* **2008**, *72*, 684–689. [CrossRef] [PubMed]
34. El Aamrani, F.Z.; Kumar, A.; Beyer, L.; Cortina, J.L.; Sastre, A.M. Uphill permeation model of gold(III) and its separation from base metals using thioures derivatives as ionophores across a liquid membrane. *Hydrometallurgy* **1998**, *50*, 315–330. [CrossRef]
35. Gupta, S.K.; Rathore, N.S.; Sonawane, J.V.; Pabby, A.K.; Janardan, P.; Changrani, R.D.; Dey, P.K. Dispersion-free solvent extraction of U(VI) in macro amount from nitric acid solutions using hollow fiber contactors. *J. Membr. Sci.* **2007**, *300*, 131–136. [CrossRef]
36. Bromberg, L.; Levin, G.; Libman, J.; Shanzer, A. A novel tetradentate hydroxamate as ion carrier in liquid membranes. *J. Membr. Sci.* **1992**, *69*, 143–153. [CrossRef]
37. Sastre, A.M.; Madi, A.; Cortina, J.L.; Miralles, N. Modelling of mass transfer in facilitated supported liquid membrane transport of gold(III) using phospholene derivatives as carriers. *J. Membr. Sci.* **1998**, *139*, 57–65. [CrossRef]
38. Haghighi, H.K.; Irannajad, M.; Fortuny, A.; Sastre, A.M. Mathematical modeling on non-dispersive extraction of germanium from aqueous solutions using Aliquat 336. *Water Sci. Technol.* **2018**, *78*, 2489–2499. [CrossRef] [PubMed]
39. Alguacil, F.J. Mechanistic investigation of facilitated transport of gold(III) from HCl media using ionic liquid Cyphos IL102 as carrier across a supported liquid membrane. *Gold Bull.* **2019**, *52*, 145–151. [CrossRef]
40. Huang, T.-C.; Juang, R.-S. Rate and mechanism of divalent metal transport through supported liquid membrane containing di(2-ethylhexyl) phosphoric acid as a mobile carrier. *J. Chem. Technol. Biotechnol.* **1998**, *42*, 3–17. [CrossRef]
41. De Gyves, J.; De San Miguel, E.R. Metals separations by supported liquid membranes. *Ind. Eng. Chem. Res.* **1999**, *38*, 2182–2202. [CrossRef]
42. Alguacil, F.J.; Adeva, P.; Alonso, M. Processing of residual gold(III) solutions via ion exchange. *Gold. Bull.* **2005**, *38*, 9–13. [CrossRef]

43. Oestreicher, V.; García, C.S.; Soler-Illia, G.J.A.A.; Angelomé, P.C. Gold recycling at laboratory scale: From nanowaste to nanospheres. *ChemSusChem* **2019**, *12*, 4882–4888. [CrossRef] [PubMed]
44. Layek, K. Hydroxyapatite supported gold nanoparticles catalyzed efficient catalysis for the reduction of nitroarenes and degradation of azo dyes. *Catal. Surv. Asia* **2024**, *27*, 349–362. [CrossRef]
45. Cheng, C.-W.; Lee, S.-Y.; Zhan, S.-Q.; Huang, C.-L.; Chen, T.-Y.; Yuan, J.-M.P.; Huang, S.-T.; Chiu, C.-M.; Liang, J.-Y. The effect of photolysis of sodium citrate treated with gold chloride using coloured light on the generation of gold nanoparticles and the repression of WiDr colon cancer cells. *J. Photochem. Photobiol. B Biol.* **2024**, *251*, 112844. [CrossRef] [PubMed]
46. Hiral, V.; Kokila, P.; Jyotindra, M. Biogenic synthesis of gold nanoparticles using bark extract of Bauhinia variegata: Antibacterial and in vitro anticancer study. *Res. J. Chem. Environ.* **2024**, *28*, 48–56. [CrossRef]
47. Ajayi, R.F.; Nqunqa, S.; Ngema, N.P.P.; Barry, S.C.L.; Feleni, U.; Mulaudzi, T. UV–Vis detection of *E. coli* 0157:H7 using *Vitis vinifera* and *Musa paradaisica* modified Au-NPs. *MethodsX* **2024**, *12*, 102522. [CrossRef]